Electrode Modification. Application in Organic Electrocatalysis

Nicolas Alonso-Vante, Kouakou Boniface Kokoh

Electrode Modification. Application in Organic Electrocatalysis

Nicolas ALONSO-VANTE and Kouakou Boniface KOKOH.

Laboratory of Electrocatalysis, LACCO, UMR-CNRS 6503, Department of Chemistry, University of Poitiers, F-86022 Poitiers, cedex, France.

Email: boniface.kokoh@univ-poitiers.fr; Nicolas.alonso-vante@univ-poitiers.fr

Table of content

1. Introduction

The electrochemical processes is determined by the law of Faraday according to which the quantity of reagent converted electrochemically is proportional to the current that crosses the surface of the electrode, and by the residual current capacitance. However, the electrochemical reaction is, essentially a heterogeneous process, and for thermodynamic and kinetic reasons, the reaction is possible in a certain domain of potential onto a defined electrode surface. It comprises several elementary processes, namely: mass transport of the reactive species toward the electrode, adsorption on an active site, exchange of electrons, possible chemical reaction, desorption, then mass transport from the electrode toward the solution, which describes the global reaction, as depicted in Figure 1.

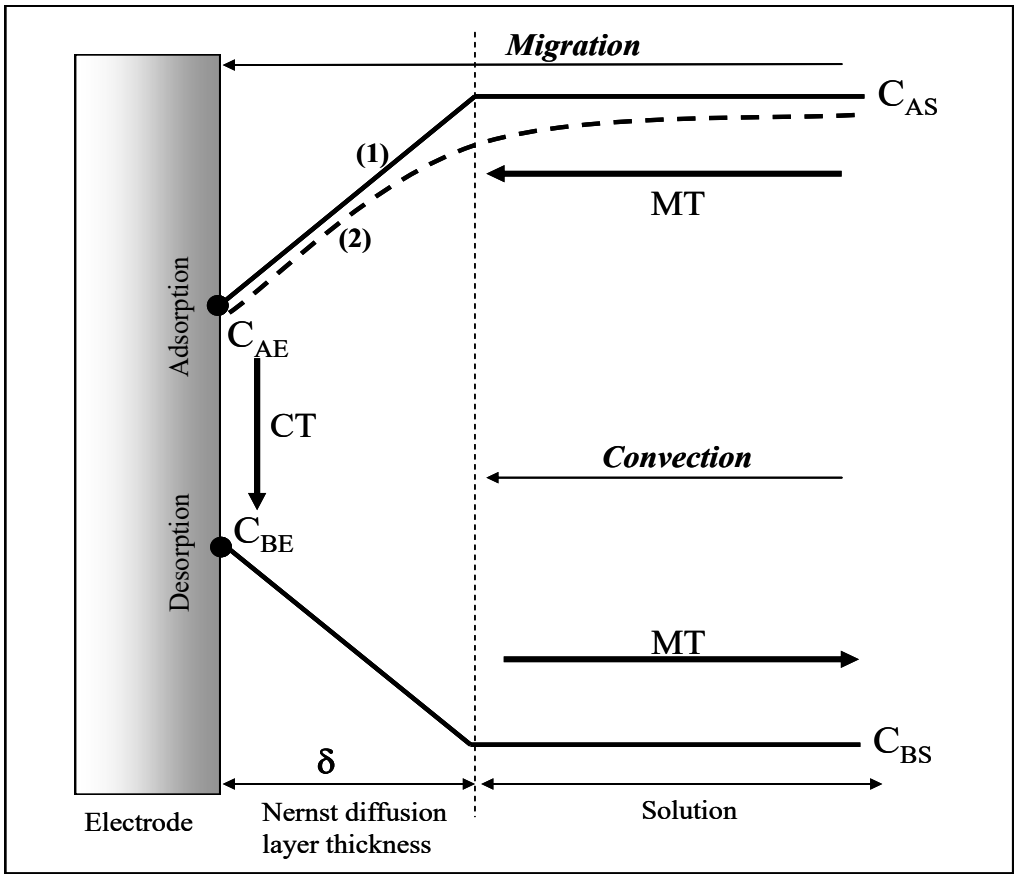

Figure 1: Schematic representation of an electrode-solution interface. MT: mass transport; CT: charge transfer; C_{AS} and C_{BS}: concentration of A and B in a bulk solution; C_{AE} and C_{BE}: concentration of A and B at the electrode surface.

Electrocatalysis is the interfacing science between liquid phase heterogeneous catalysis and electrochemistry. According to a general definition, electrocatalysis may be defined as the acceleration of an electrode reaction by a substance which is not consumed in the overall reaction. The substance is mostly the electrode itself; however the catalytic effects of other components (for instance, the solvent) may also be envisaged.[1]

If we restrict the discussion to the catalytic effect of the nature and structure of the electrode material and we consider systems with polar liquid components (for instance, water and aqueous solutions) it is relatively easy to find a link between electrocatalysis and liquid phase heterogeneous catalysis. A liquid phase heterogeneous catalytic system where an electrified interphase is formed between the solid and liquid phases should also be considered as an electrochemical system. Thus, the interphase may be envisaged as consisting of the surface regions of two phases in contact where the accumulation or depletion of free charged components can occur resulting in net charges on the phases. In such systems charged components may or may not cross the interface between the two phases. Depending on this condition electrochemists speak about unpolarizable and polarizable systems. The thermodynamic description of an electrified solid-liquid interphase is similar to that of non-ionic systems with one important difference; the description requires the introduction of electrochemical parameters: the thermodynamic charge and the electrical potential difference between the solid phase considered and the reference electrode. This means that a heterogeneous catalytic system where an electrified interphase is formed cannot be unambiguously treated ignoring the electrochemical parameters.

Electrocatalysis is a heterogeneous process which involves adsorption and chemisorption of reactants or intermediates at the interface. These phenomena are encountered, e.g., in fuel cells or inorganic electrosynthesis. The electrocatalytic activity of a given electrode for a certain reaction may be characterized by the current density at a chosen potential, which is proportional

to the specific activity, when referred to the effective active surface. As shown in Figure 2, the role of a heterogeneous catalyst is to adsorb the electroreactive species (reactant and intermediate) and to transform it into another compound readily to undergo the desired chemical transformation.

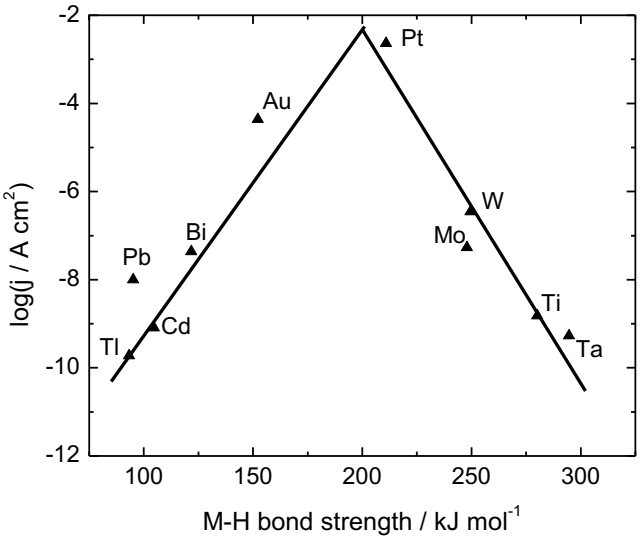

Figure 2: Volcano-shaped plot of the exchange current density for the hydrogen evolution reaction as a function of the metal-hydrogen bond energy.

Therefore, if the heat of adsorption is low the extent of adsorption will be very small. If the binding energy to the surface is too high, the adsorbed intermediate or its product may remain "attached" to the surface and effectively poison it. The "best" catalyst is thus one giving rise to an intermediate adsorption energy value.[2]

2. Multi-electron charge-transfer reactions.

The need to convert chemical energy to electricity efficiently and at low temperature has increased the development of materials with electrocatalytic activity toward multi-electron charge transfer. Reactions of technical relevance are, e.g., the cathodic processes, such as, the

oxygen reduction reaction (ORR),[3] and anodic processes such as, small organic (R-OH, where R = CH_3-[4-13] or CH_3CH-[14-18]), sugars.[19-21] These complex electrochemical processes are useful in low temperature systems such as the direct methanol fuel cell (DMFC)[22-23] or bio-fuel cell systems.[24-26]

2.1 Oxygen reduction reaction (ORR).- The marked irreversibility of this electrochemical process, which leads to excessive voltage losses at reasonable temperatures, has complicated the mechanistic studies. Indeed, in aqueous solvents molecular oxygen requires a strong interaction with the electrode surface for the reaction to proceed at a reasonable rate, with a number of elementary steps involving various reaction intermediates. The reduction can proceed either via formation of water (four-electrons), or hydrogen peroxide (two-electrons). Studies of the ORR in acid medium on platinum at rotating ring-disk electrodes[27] reported that the mechanism proposed by Damjanovic et al.[28] appears suitable. A similar scheme adapted for alkaline medium was later reported by Wroblowa et al.[29] Furthermore, the ORR is also sensitive to the electrolyte nature (adsorbed anions),[27, 30-31] to the structure of surface of the electrode materials,[31-35] and to the particle size.[30-31, 34-36]

This electrochemical cathodic process is the complementary reaction aiming at developing an energy converting system with the anodic process based on an organic fuel such as glucose (see next sections). However, if the electrode material is based on platinum, the anodic process is affected by the nature of the fuel, other than hydrogen, inducing an anodic overpotential "η_a". Efforts to reduce the overpotential at the cathode as well as the anode reactions are focused on novel material synthesis. A recent review on cluster-like materials, obtained via the carbonyl chemical route, to enhance selectivity and reactivity of ORR, has been recently reported.[37]

2.2 Sugar oxidation reaction (SOR).- Glucose is an example of a reducing carbohydrate. It

becomes a pyranose when dissolving in aqueous solution by hemiacetalization (a chemical reaction between the aldehydic group and the secondary alcohol in C5 position):

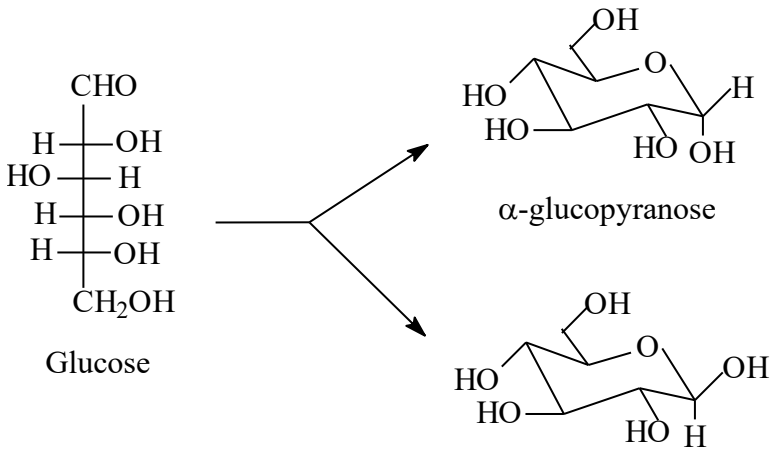

(1)

Among these two anomeric forms, β-glucopyranose is described as the electroreactive species of glucose.[38-39] The oxidation of the carbon in the C1-position on a noble electrode material such as Pt or Au is representative of reducing sugars, which proceeds by dehydrogenation:

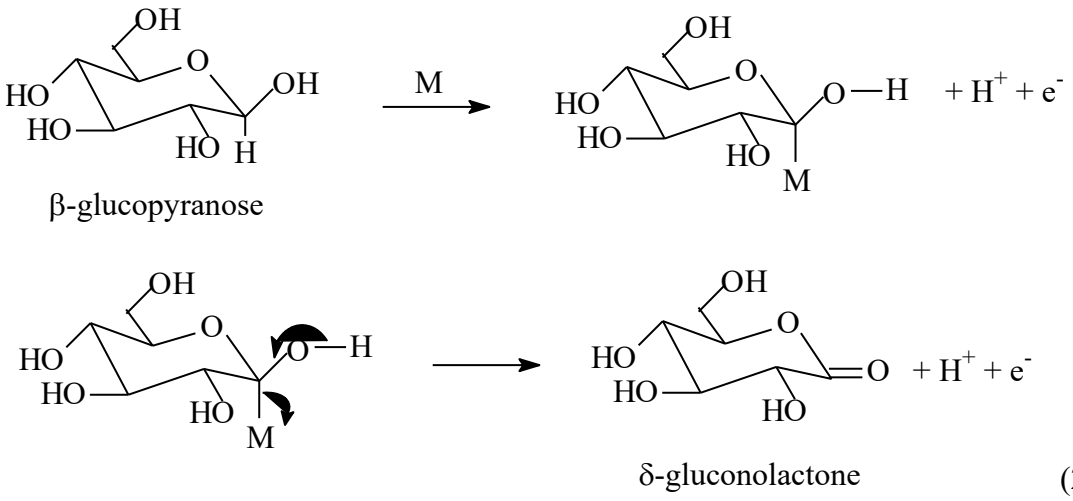

(2)

where M represents Pt or Au surface electrode atoms.

The lactone undergoes hydrolysis in solution to form the corresponding aldonic acid, that is, here, gluconic acid, as follows:

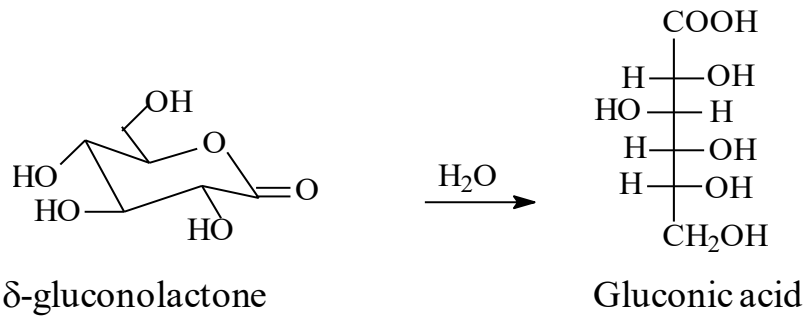

δ-gluconolactone Gluconic acid (3)

The electrocatalytic oxidation of the primary alcohol (in C6 position) is similar to the reaction mechanism which is well known for methanol. Therefore, the transformation of gluconic acid into glucaric acid can be written as follows:

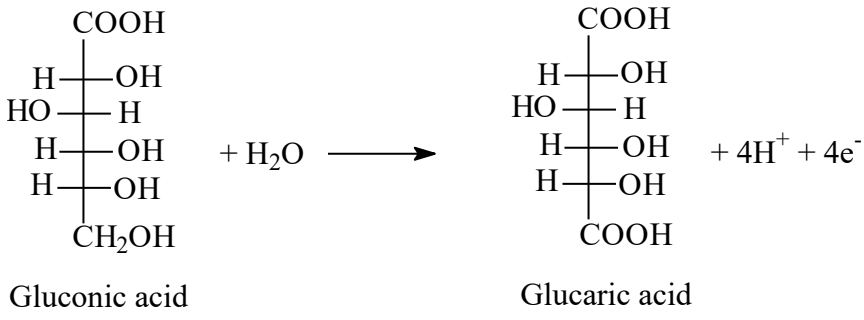

Gluconic acid Glucaric acid (4)

3. Electrode Surface modification for electrocatalysis

3.1 Metal adatoms: platinum and gold electrodes

3.1.1 Characterization of the electrode surface.- Cyclic voltammetry is a widely used electrochemical technique which allows the investigation of the transient reactions occurring on the electrode surface when the potential applied to the electrode is varied linearly and repetitively at a constant sweep rate between two given suitable limits. The steady-state current-

potential curves or voltammograms provide direct information as to the adsorption-desorption processes and allow to estimate the catalytic properties of the electrode surface.

The voltammogram of a platinum electrode recorded at 25 °C in 0.5 M H_2SO_4 between a lower limit (E_C = 0.05 V *vs*. RHE) and an upper limit (E_A = 1.5 V *vs*. RHE) displays three regions according to the applied potential (Figure 3). Region I at lower potentials is associated with the adsorption (reduction peaks)-desorption (oxidation peaks) of hydrogen, which is very sensitive to the crystallographic orientation of the Pt surface mainly constituted of (110), (100) and (111) faces.

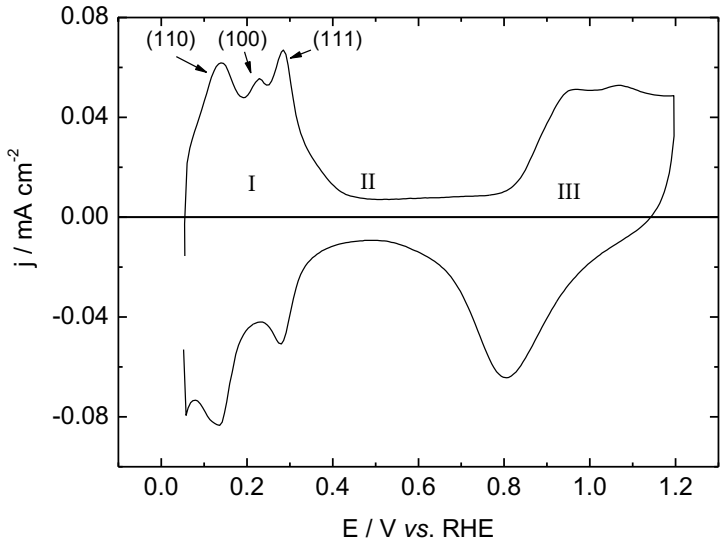

Figure 3: Voltammogram of a Pt electrode in 0.5 M H_2SO_4 at 50 mV s^{-1} and 25 °C.

Region III at higher potentials reveals the adsorption (oxidation peaks)-desorption (reduction peak) of hydroxyl and oxygenated species at the electrode surface.[40-42] Between them the double layer region II, where no electrochemical reaction occurs, is characterized by a small current associated with the charge and discharge of the double layer capacitance.

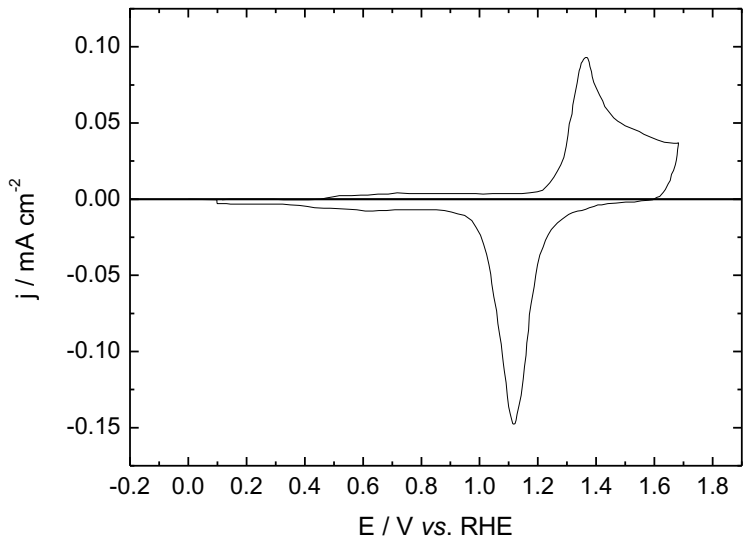

Figure 4: Voltammogram of a gold electrode in 0.5 M H_2SO_4 at 50 mV s^{-1} and 25 °C.

Considering now a gold electrode, the voltammogram recorded, under the same experimental conditions (0.5 M H_2SO_4, 25 °C), is relatively simple, the hydrogen region having disappeared (Figure 4). The double layer region is remarkably spread out in a potential interval of 0.05 to 1.3 V *vs*. RHE. The oxygen region is characterized by the occurrence of several adsorption peaks and usually a single desorption peak at *ca*. 1.1 V *vs*. RHE.

When the same experiments are performed in alkaline medium, 0.1 M NaOH, the main features of both voltammograms remain unchanged. However, it is interesting to point out the existence of important currents in the double layer region for both electrodes. These currents arise from Faradaic processes associated with the oxygen region, which begin earlier in alkaline medium, particularly for the gold electrode, where the onset of the adsorption of oxygenated species begins at 0.4 V *vs*. RHE (Figure 4). Although the voltammetric investigation does not allow one to identify this kind of adsorbed species, it is reasonable to think that this current is related to earlier OH adsorption, as far as this process is supposed to be favored in alkaline

medium. Therefore, this layer will necessarily affect the catalytic properties of a gold electrode surface in alkaline solution, as compared with its behavior in acid medium, and explain part of the results which will be given below.

CO-stripping voltammetry is also used for the calculation of the true electrode surface area (Figure 5). CO adsorption on the electrode was carried out by bubbling CO gas for 2 min at 0.05 V *vs*. RHE. Thereafter, CO was removed from the solution by bubbling nitrogen for 15 min.

The effective electroactive surface may be determined directly by the voltammogram in evaluating the quantity of electricity involved in the adsorption-desorption of hydrogen (region I). The quantity of electricity is obtained by integration of the current-potential curves, because the potential varies linearly with time. The active surface area (S = 0.56 cm^2) is then calculated from the charge under the hydrogen underpotential-deposited (UPD) peaks, which needs 210 $\mu C\ cm^{-2}$, as follows:

$$Pt + H^+ + e^- \longrightarrow Pt\text{—}H_{ads} \qquad (5)$$

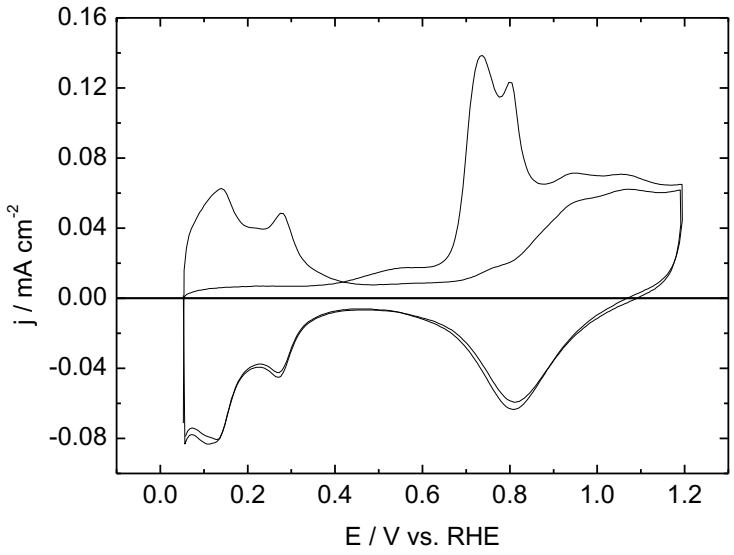

Figure 5: CO stripping on a Pt electrode in 0.5 M H_2SO_4 at 50 mV s^{-1}. All the electrochemical experiments were carried out at 21±1 °C. The electrolytic solution was deoxygenated by bubbling nitrogen during 15 min.

The charge involved in the CO oxidation allowed the determination of the surface areas of platinum. Assuming that the monolayer of adsorbed CO needs 420 μC cm^{-2} for its oxidation to CO_2 on the Pt surface:[43]

$$Pt + H_2O \longrightarrow Pt\text{—}OH_{ads} + H^+ + e^- \quad (6)$$

$$Pt\text{—}CO_{ads} + Pt\text{—}OH_{ads} \longrightarrow CO_2 + 2Pt + H^+ + e^- \quad (7)$$

The quantity of electricity involved in this reaction allowed to determine the active Pt surface (0.52 cm^2).

Surface composition of a catalyst can also be determined in alkaline medium using the oxide reaction formation at a given potential. Figure 6 shows a cyclic voltammogram of $Pt_{50}Au_{50}$

catalyst dispersed on carbon XC-72 Vulcan. The charge associated to reduce the oxide species can be used to determine the surface composition.

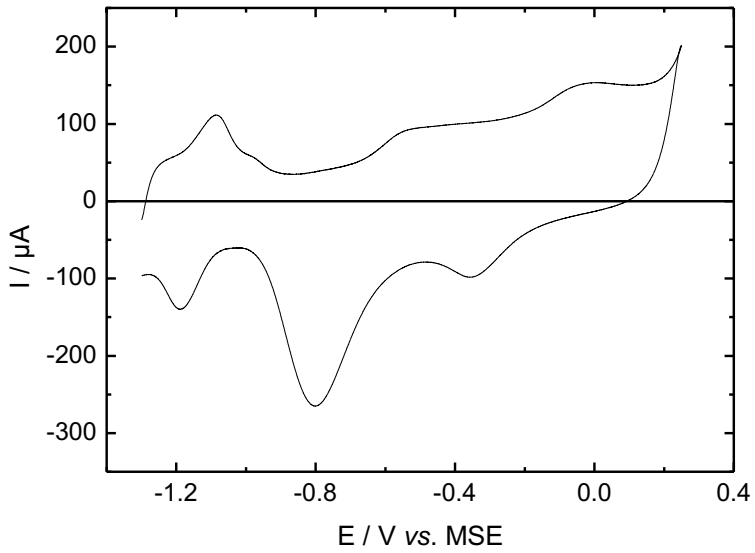

Figure 6: Voltammogram of $Au_{50}Pt_{50}$ nanoparticles deposited on a carbon rotating disk electrode recorded in 0.1M NaOH at 50 mV s^{-1} and 25 °C.

The peak around -0.38 V *vs*. MSE, during the negative sweep, is associated to gold species whereas the one at -0.8 V *vs*. MSE corresponds to platinum species. For pure catalysts, with an upper potential limit of +0.25 V *vs*. MSE, the charge values of 493 and 543 $\mu C.cm^{-2}$ were obtained for Pt and Au, respectively (Figure 7).[44-45]

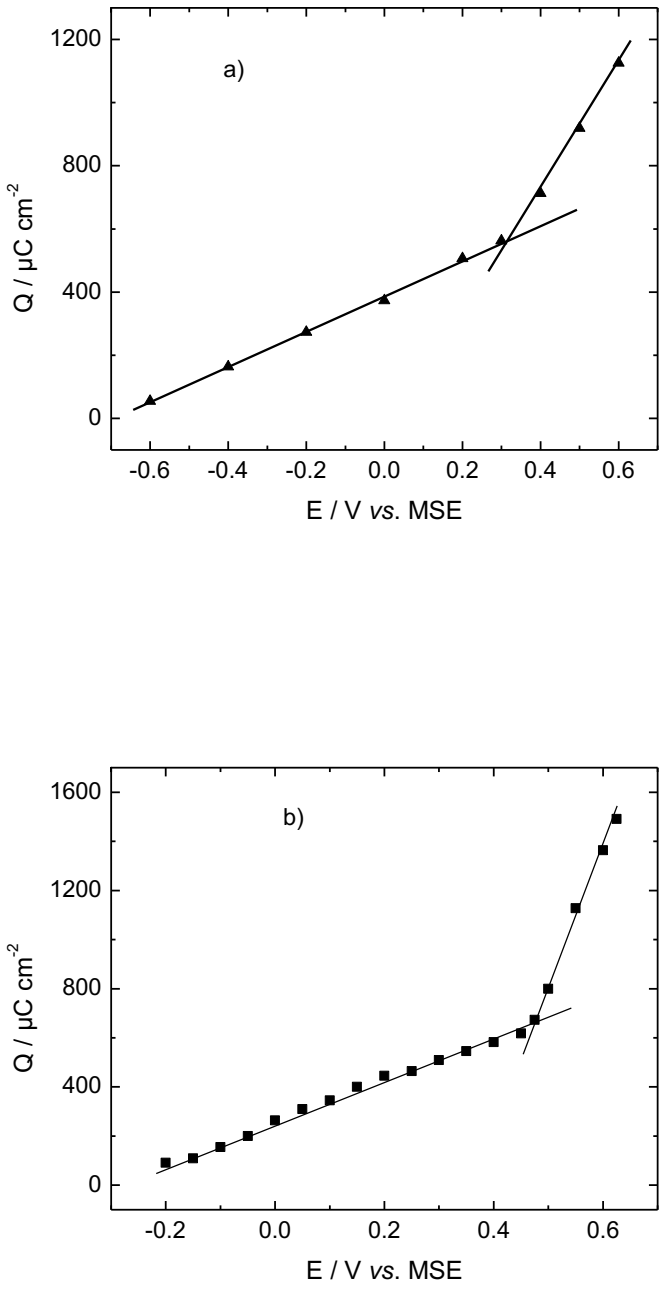

Figure 7: Quantity of electricity involved as function of the upper potential limit of voltammograms recorded in alkaline medium 0.1 M NaOH and at 25 °C. (a) on a Pt electrode. (b) on a Au electrode.

The atomic content of the Pt-Au nanoparticles can be deduced as follows:

$$x = \frac{S_{Au}}{S_{Au} + S_{Pt}} \times 100 \quad (8)$$

where x represents the Au content, S_{Au} and S_{Pt} are the electrode surface covered by gold and platinum oxides, respectively. The active surface area due to the surface composition of the catalyst was estimated to 0.5 cm^2, which represents 18.4% of the Au content in $Pt_{50}Au_{50}$.

3.1.2 Underpotential deposition of metal ions.- The modification of surface catalytic properties by the deposition of metal adatoms has been studied extensively in the field of electrocatalysis.[46-60] The main and most common metals used as adatoms have low energy of adsorption (cf. Figure 2). Adatoms are considered as a means to enhance the catalytic activity of the electrode surface. Underpotential deposition is the process of the deposition of submonolayer amounts of metal ions (M^{z+}) on an inert foreign metal (M) support from a solution considered at more positive potentials than the corresponding M^{z+}/M equilibrium potential.

The electrocatalytic oxidation of organic molecules has been studied very extensively using various supports and adatoms. There are several proposed mechanisms in the literature to interpret the role of adatoms. It is assumed, for instance, that adatoms block the poison formation not leaving enough space for these reactions. According to another hypothesis, adatoms act as redox intermediates. Independently from the explanation, it is a fact that very often a significant enhancement of the catalytic activity can be observed, and these results could provide a very useful information for liquid phase catalytic reactions.[61]

4. Electrosynthesis in aqueous medium

4.1 Electrooxidation of carbohydrates and alcohols

As a first attempt in applying electrocatalysis to the valorization of carbohydrates, the regioselective electrooxidation of monosaccharides (glucose) and disaccharides such as sucrose and lactose, was investigated. Corresponding acids or ketones keeping their initial skeleton are of interest in the pharmaceutical and detergent branches. Mono and dicarboxylic acid of disaccharides are important intermediates in the selective synthesis of ester and amides of carbohydrates, which can be used as biodegradable tensioactive compounds.

The oxidation reaction of different sugars was carried out in alkaline medium because:

- they are not electroreactive in acid medium.
- the disaccharides such as sucrose undergo inversion reaction in acid medium implying the cleavage of the C-O-C glycosidic bond.
- The carbohydrates present a fragile structure so that the removal of the aqueous solution by evaporation on vacuum degrades the molecules. However, at the end of the oxidation process, the electrolyte is easily neutralized with a cation exchange resin (Amberlite 200, which allows a lyophilization of the aqueous solution free from inorganic species.

4.1.1 Electrochemical oxidation of ascorbic acid at a platinum electrode

Investigation was made into the transport characteristics of ascorbic acid (AA). Cyclic voltammograms of 10 mM AA at different scan rates were recorded at platinum (Figure 8) without stirring the solution with the rotating disk electrode (RDE).

If the electrooxidation of AA at the Platinum electrode is controlled solely by the mass transfer process in the solution (Figure 9), the relationship between the maximum current density at the maximum potential should obey the Randles-Sevcik law

$$I_P = 0.4463nF\sqrt{nF/RT} \times SD^{1/2}C_{AA}\sqrt{v} \qquad (9)$$

where D, S and C_{AA} are the diffusion coefficient, the surface area of the electrode and the concentration of AA in the solution, respectively.

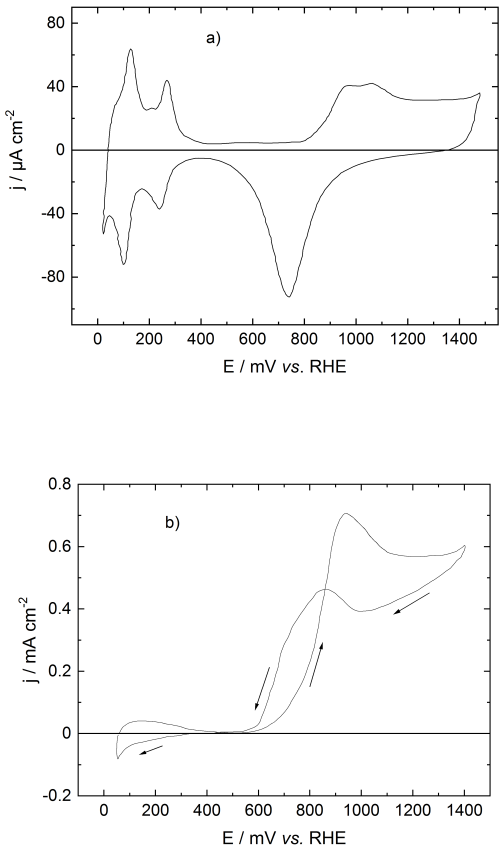

Figure 8: Cyclic voltammograms of Pt a supporting electrolyte 0.5 M H_2SO_4 (a) and in the presence of 10 mM ascorbic acid (b) with a scan rate of 0.01 V s^{-1} at 20 °C.

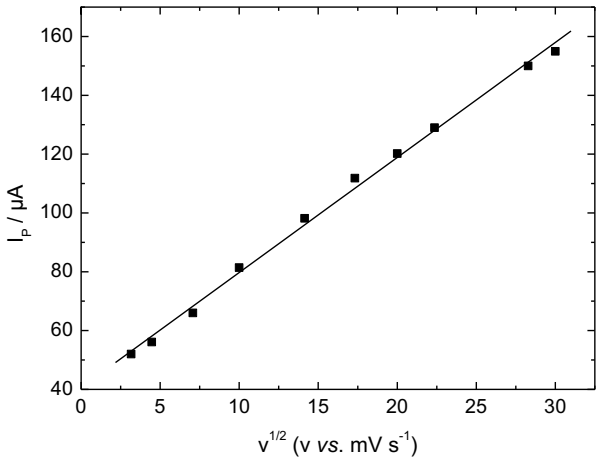

Figure 9: Plot of I_p versus $v^{1/2}$ for the electrooxidation of AA on a Pt electrode in 0.1 M H_2SO_4

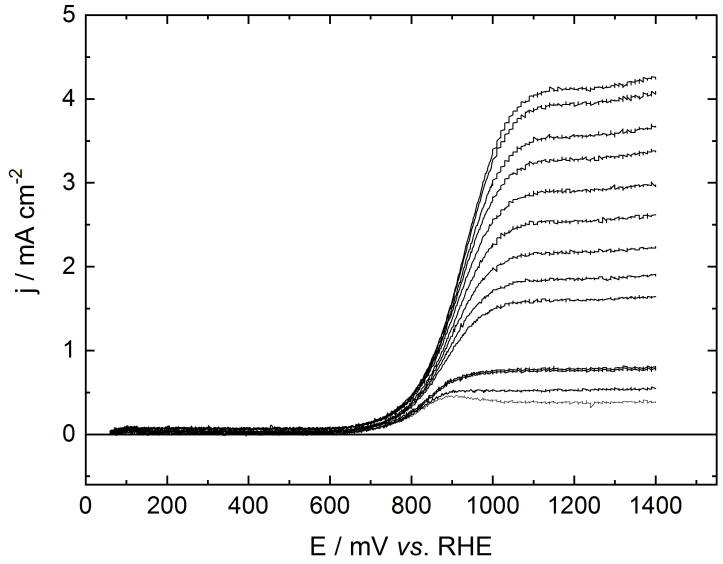

Figure 10: Current density-potential profiles at a RDE Pt electrode with 10 mM AA in 0.5 M H_2SO_4 at different values of rotation rate ω (49, 100, 490, 700, 900, 1200, 1600, 2000, 2500, 2900, 3600, and 4000 rpm) at 0.01 V s^{-1}.

In order to determine the kinetic parameters of the reaction corrected from diffusion phenomenon, a voltammetric investigation was pursued with a rotating platinum ring disk electrode. Figure 10 represents current density-potential curves obtained for different rotation speeds and for the positive variations of potential. It appears that the current density of the rotating disk increases with the rotation rate.

For reactions controlled by both activation and mass transfer, the total current density is expressed as follows and known as Koutecky-Levich plots:

$$\frac{1}{j} = \frac{1}{j_k} + \frac{1}{j_L} \qquad (10)$$

where j_L is the current density due to mass transfer (according to hypothesis of Nernst double layer) ; j_k is the kinetic current density, that is, the oxidation current obtained in the absence of

mass transfer.

As j_L is proportional to $\Omega^{1/2}$ (Ω being the rotation rate), the current density of the disk is related to the rotation rate according to:

$$\frac{1}{j} = \frac{1}{j_k} + \frac{1}{B\sqrt{\Omega}} \quad (11)$$

B is given by

$$B = 0.2nF(D_{AA})^{2/3}\nu^{-1/6}C_{AA} \quad (12)$$

where *n* is the number of electrons transferred per molecule of AA

D_{AA} is the diffusion coefficient of AA, C_{AA} is its concentration

v, the kinematics viscosity of the solvent (v_{H2SO4} = 1.009 × 10^{-2} cm^{-2} s^{-1}).[61] Therefore, as shown by Levich, a plot of 1/j *vs.* $\Omega^{-1/2}$ should be linear (Figure 11). Its slope allowed to evaluate the value of the diffusion coefficient of AA for 6.5 × 10^{-6} cm^2 s^{-1}.

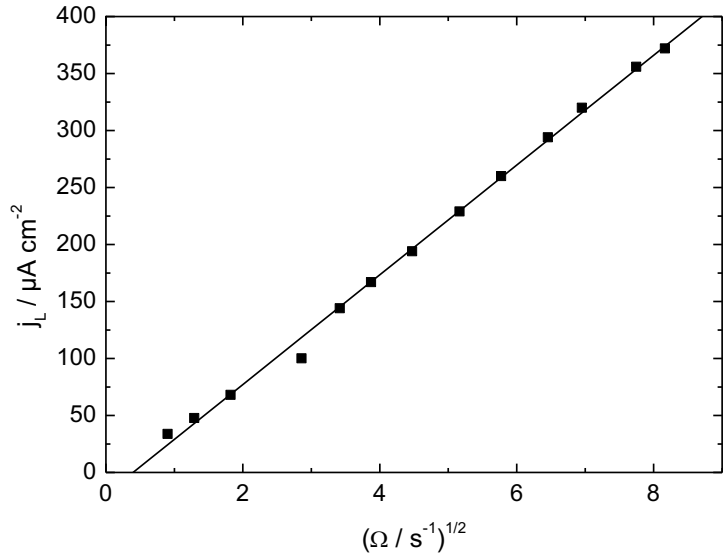

Figure 11: Levich plot of the main data in Figure10 at E = 1.2 V *vs*. RHE.

4.1.2 Electrooxidation of glucose

4.1.2.1 Polarimetric measurements.- The specific rotation angle [α] is related to the experimental rotation angle of light α through the so-called Biot and Savart law:

$$[\alpha] = \frac{100\alpha}{l \times c} \tag{13}$$

where *l* is the length of the polarimetric tube thermostatted at 2 °C, expressed in dm, and C is the concentration of the active substance, expressed in g per 100 cm^3. [α] and α are expressed in degrees and decimal fractions of α degree.

Different solutions of glucose were characterized by polarimetry, referring to the specific rotation angles of the two glucose anomers, namely + 112° for the α form and + 18.7° for the β form. Measuring the specific rotation angle [α] of the solution is thus a way of determining the proportion of each form and thus of determining which anomeric form prevails. For instance, the percentage of the β form can be calculated simply by:

$$\%\beta = \frac{[\alpha] - 112}{18.7 - 112} \times 100 \tag{14}$$

The evolution of the specific rotation angle in acid medium (pH 1) at 2 °C is given in Figure 8 for the three solutions prepared from the initial "α", "β" and "commercial" D-glucose (Pro-analysis from Merck). In each case, the equilibrium is attained slowly. After 5 hours the β form which amounts to about 71% of β-D-glucose in solution, exhibits the highest stability. At the same time, α and D-glucose form solutions containing only 52 and 56% of α-D-glucose, respectively.

In neutral medium (Figure 9), both α and β forms exhibit a stability, but it should be noted that the β form appears to be more stable (95% in solution) and that D-glucose leads to solutions where the α form is dominant (73% in solution).

The influence of the alkaline medium is interesting (Figure 14). It is remarkable that an equilibrium is reached very quickly (first measurement at t = 5 min after glucose dissolution). Each solution contains *ca*. 80% of the β form which is unstable in alkaline solution.

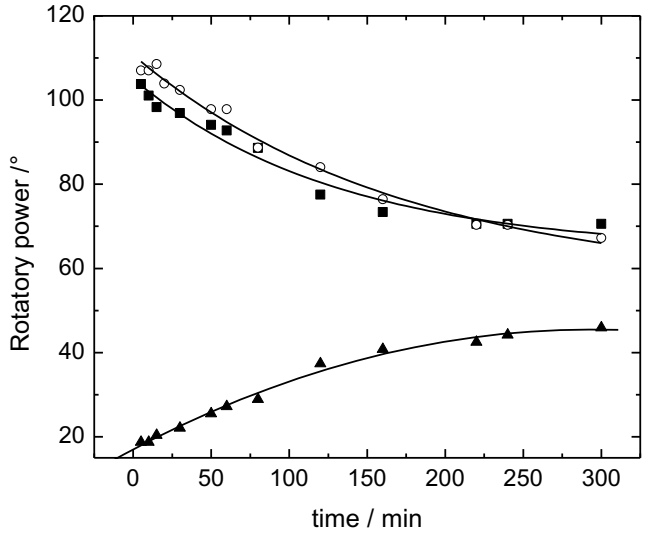

Figure 12: Evolution of the rotatory power for α-glucose (○), β-glucose (▲) and D-glucose (■) in acid medium (0.1M $HClO_4$).

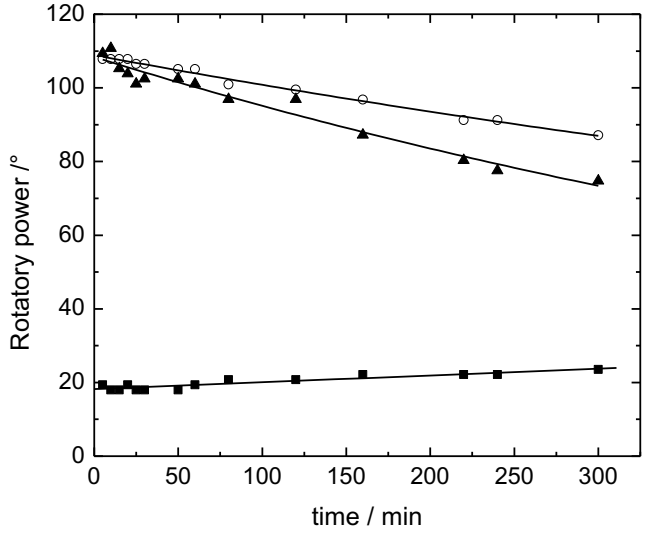

Figure 13: Evolution of the rotatory power for α-glucose (○), β-glucose (▲) and D-glucose (■) in acid water.

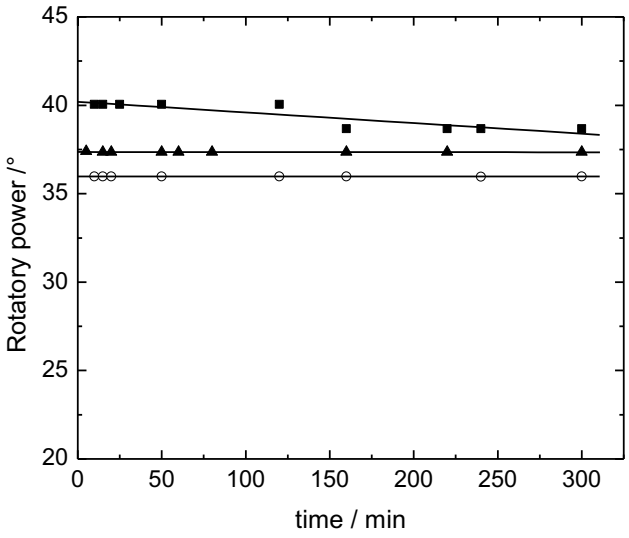

Figure 14: Evolution of the rotatory power for α-glucose (○), β-glucose (▲) and D-glucose (▪) in alkaline medium (0.1M NaOH).

4.1.2.1 Electrochemical measurements - Figure 15 represents the voltammograms of platinum in alkaline medium (0.1 M NaOH). In agreement with polarimetric experiments, indicating that the composition of the three solutions is almost the same in alkaline solution, the voltammograms are similar and correspond to those previously described for D-glucose under the same conditions. However, if we can conclude that β-glucose, predominant in solution is reactive, it is more difficult to say the same for the α form which is always the minor component (*ca*. 20% in solution).

The situation is different in acid medium and the solutions prepared at low temperature retain the α and β predominant forms long enough to obtain evidence for a possible difference in reactivity between the two anomers.

The oxidation reaction of glucose at 0.3 V *vs*. RHE was carried out during long-term electrolysis. The activity of the Pt electrode decreased quickly because of poisoning adsorbed

intermediates, a pulse potential set at 1.4 V was added to the time-program in order to reactivate *in situ* the Platinum surface.

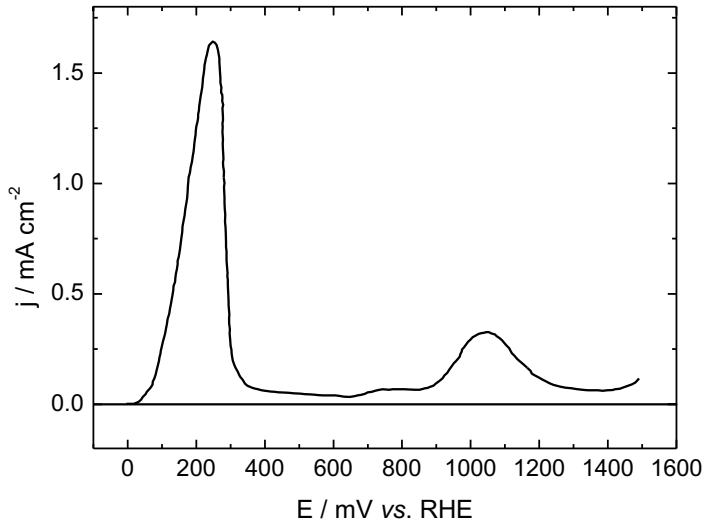

Figure 15: Anodic sweep curve of a Pt electrode in alkaline medium (0.1M NaOH) recorded at 50 mV s^{-1} and at 2 °C, with 0.1 M D-glucose.

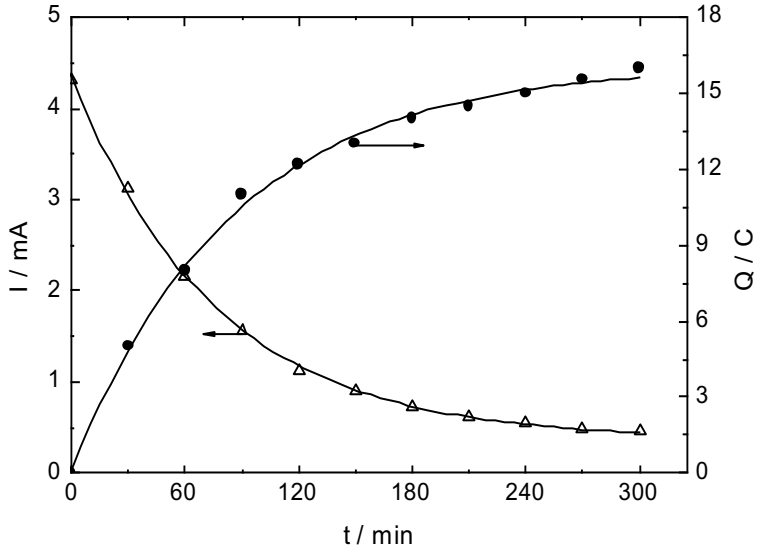

Figure 16: Evolution of the current intensity and the quantity of electricity involved during electrolysis of 0.1M glucose in 0.1M NaOH at 0.3 V *vs*. RHE and 2 °C.

Figure 16 shows the variations of the current intensity and the charge involved during the oxidation reaction of glucose on a Pt electrode. At the end of electrolysis gluconate was detected

by ionic chromatography as the main oxidation product of glucose, that is, the chemical transformation processes in alkaline medium (epimerization and interconversion) is nearly stopped at low temperature. The following reaction mechanism of dehydrogenation of glucose is commonly proposed:[39, 62-64]

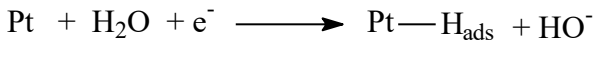

(15)

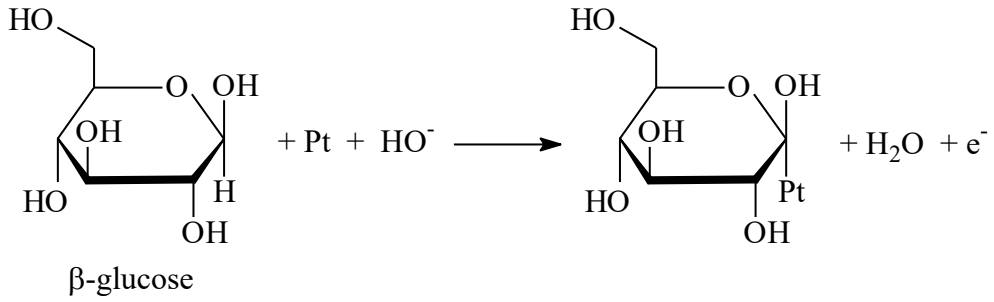

(16)

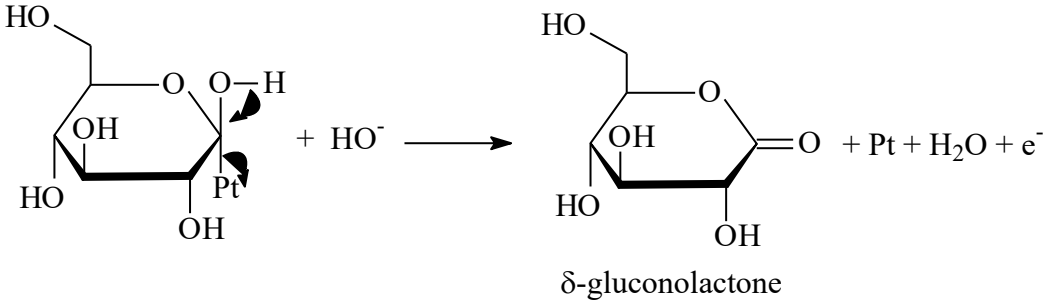

(17)

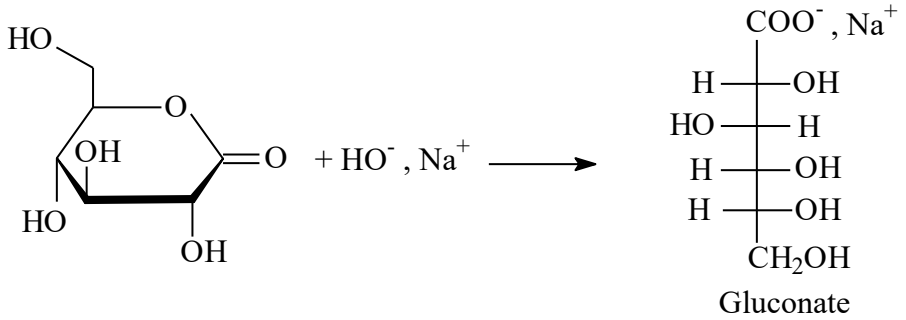

(18)

The electrolytic solution was neutralized with a cation exchange resin (Amberlite 200 from Sigma). The aqueous solution, free from inorganic ions, was then lyophilized, and the crystals obtained were trimethylsilylated for analysis on GC/MS:[1]

- Main fragments of δ-lactone m/e: 377; 361; 320; 271; 259; 243; 220; 204; 189; 169; 157; 147; 129
- Main fragments of glucose m/e: 393; 361; 317; 305; 271; 243; 217; 204; 191; 147; 129

As a result, β-glucose is the major configuration in alkaline solution at low temperature. Its most planar approach of the anomeric form of the molecule to the electrode surface facilitates its dehydrogenation at low potentials to δ-gluconolactone; the latter reaction product undergoes hydrolysis in the bulk solution to gluconate as shown by Largeaud et al. using *in situ* reflectance infrared spectroscopy.[65]

4.1.3 On platinum-adatoms.- Because of the poisoning phenomena occurring in long-term electrolysis and in order to maintain the electrode activity at a sufficient level, the oxidation reaction of carbohydrates was carried out using an optimized triple-pulse potential program (Figure 17).

[1] Gas chromatography was equipped with a DB-5, 95% dimethyl 5% diphenyl polysiloxane bounded capillary column. It was combined with a Mass Spectrometer (ITS 40 Finnigan Matt).

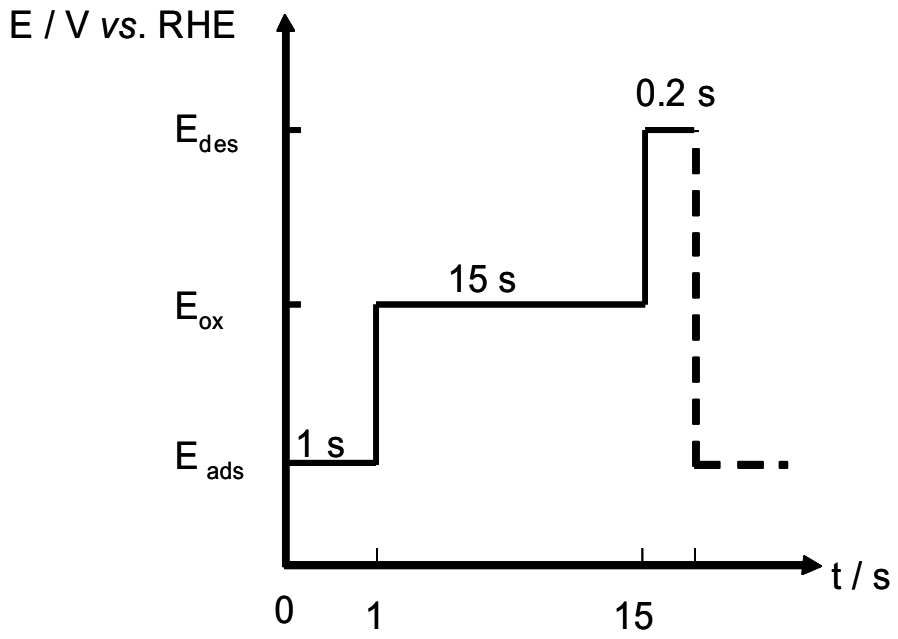

Figure 17: Potential program used for long-time electrolysis of carbohydrates.

It consists in controlling the oxidation potential which, by itself, is a parameter of selectivity. The oxidation plateau was applied during the long time of the sequence in a potential range corresponding to the maximum of electrode activity (E = 0.7 V *vs*. RHE). Then the electrode surface was reactivated by clearing out the poisoning species by oxidation at higher a potential during 0.2 s. The third pulse was set during 1 s in the hydrogen region, allowing the reduction of the surface and/or the "*in situ*" underpotential deposition of adatoms. This sequential unit program was repeated during the time of electrolysis.

Lead perchlorate and Bi nitrate were added to the electrolytic solution at $5x10^{-5}$ and 10^{-5} M, respectively to modify a Pt electrode which has a real surface area of 40 cm^2. The electrolysis cell has two identical compartments separated by an ion-exchange membrane (Nafion® 423). A $Pt_{90}Ir_{10}$ sheet and $Hg/Hg_2SO_4/SO_4^{2-}{}_{sat}$ electrode served as counter and reference electrodes, respectively.

The analysis of the reaction products was performed with an ion-exchange liquid chromatography (Dionex-4500i). It works with a ternary gradient elution and includes an ion-

exchange column (AG11+AS11) and a double detection that is, a conductimeter (for the ionisable compounds such as carboxylic acids) followed by a refractive index detector that is specifically dedicated to the D-glucose consumption.

According to the nature of the metal used as adatom to partly cover the Pt electrode surface, the oxidation route is strongly modified as shown in Schemes 1 and 2:

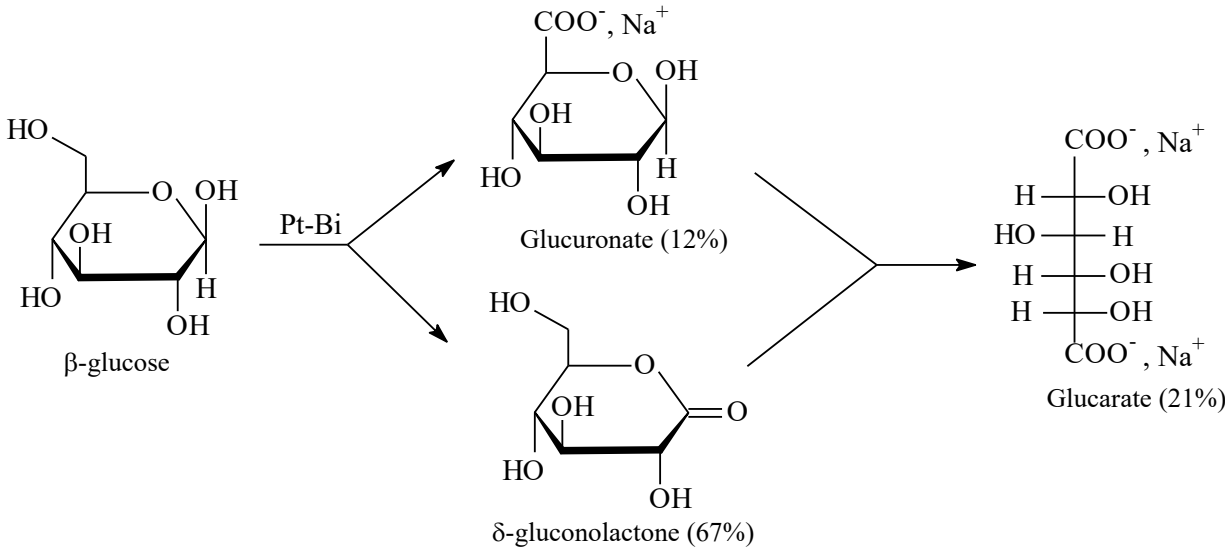

Scheme 1: Oxidation of glucose at 0.7 V *vs*. RHE in carbonate buffer on Pt electrode modified by Bi adatoms.

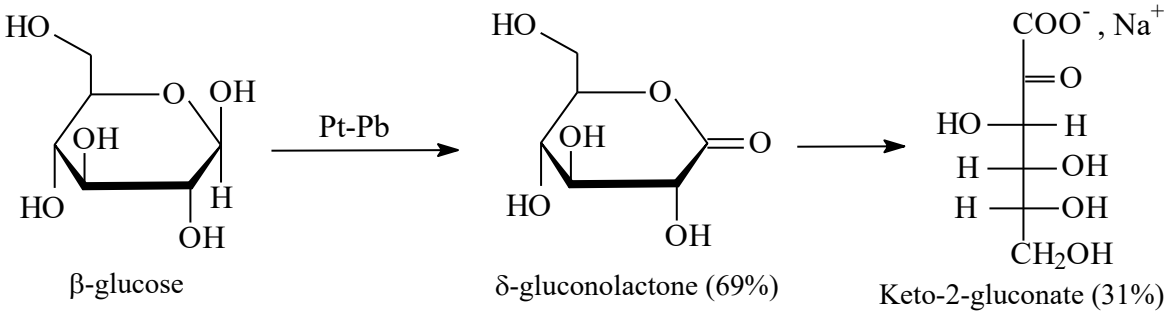

Scheme 2: Oxidation of glucose at 0.7 V *vs*. RHE in carbonate buffer on Pt electrode modified by Pb adatoms.

4.1.4 Gold-adatoms.- As shown in different works,[42, 66-72] the mechanism of glucose electrooxidation on Pt is similar to that on Au electrode. The primary and main reaction product remains glucono-δ-lactone which is transformed into gluconate by hydrolysis.

In the presence of metal adatoms, a triple-pulse potential program shown in Figure 17, is also applied during electrolysis of glucose on an Au electrode. The adsorption of adatoms (e.g., bismuth in Figure 18) occurs simultaneously with glucose dehydrogenation at the electrode surface.

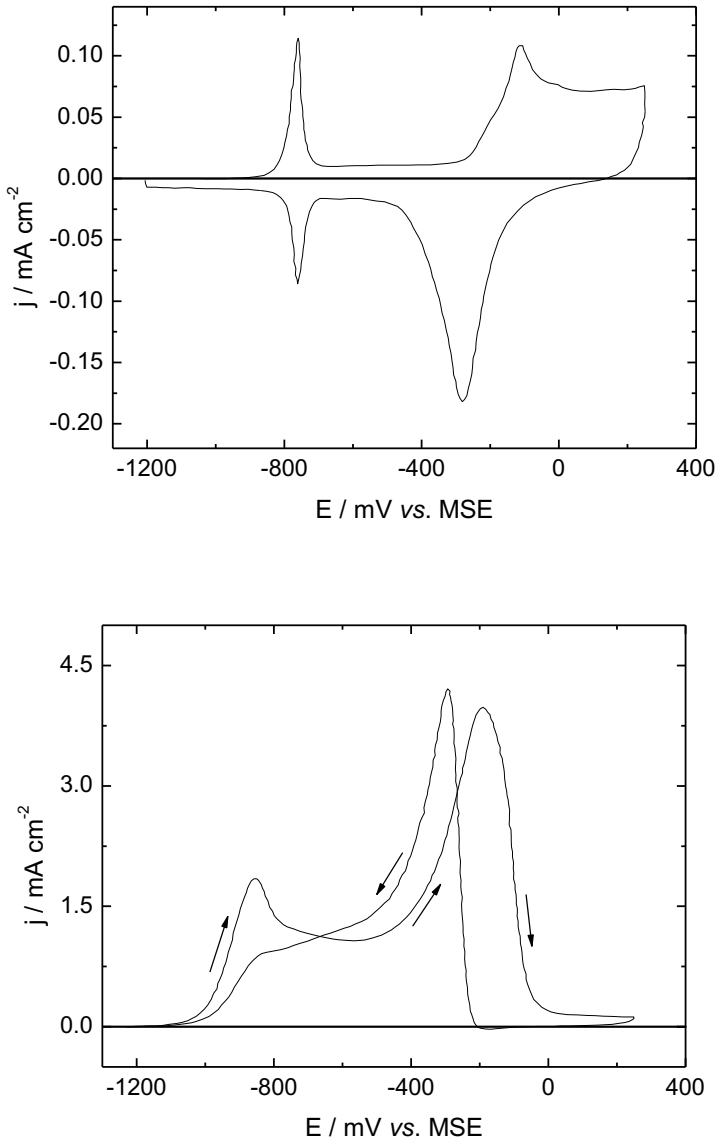

Figure 18: Voltammograms of a Au–Bi electrode in alkaline medium (0.1 M NaOH), recorded at 50 mV s^{-1} and at 22 °C.

At higher potentials (E > 0.4 V *vs*. RHE), the desorbed adatoms are quickly replaced by hydroxyl groups which could later on contribute to the surface oxidation of the organic

adsorbates. This leads us to postulate a reaction mechanism of glucose oxidation on Pt-Bi, as follows:

- At ca 0.4 V the adsorption of the metal adatoms from Bi^{3+} in solution and that of glucose at the electrode surface first occurs:

$$Au + Bi^{3+} + 3e^- \rightarrow Au\text{-}Bi_{ads} \quad (19)$$

$$Au + C_6H_{12}O_6 + HO^- \rightarrow Au(C_6H_{11}O_6)_{ads} + H_2O + e^- \quad (20)$$

At lower potentials the desorption of glucose species can lead to glucono-δ-lactone

- For $0.5 < E_{ox} < 0.9$ V, the hydroxyls necessary to the oxidation of the electrode surface competes with Bi adatoms still adsorbed. Both these adsorbates modify the organic oxidation, such as gluconate (40%) leading to the formation of keto-2-gluconate that is the second compound produced in an appreciable amount (19%):

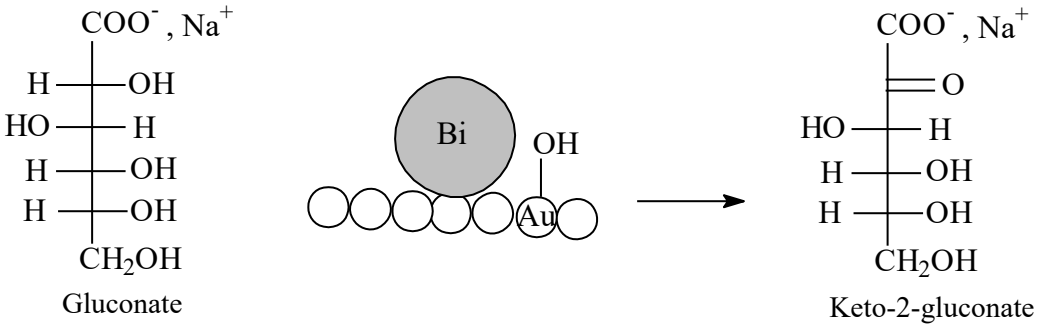

Scheme 3: Conversion of gluconate to keto-2-gluconate.

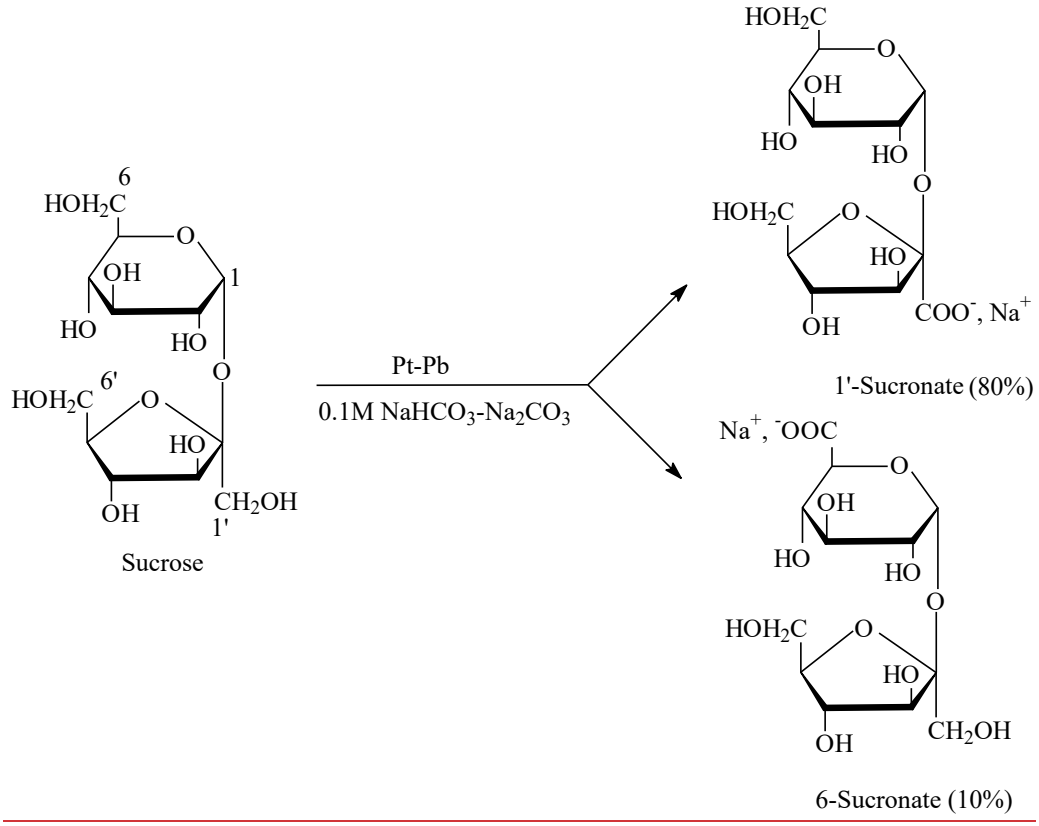

Scheme 4: Conversion of gluconate to keto-2-gluconate.

4.1.5 Electrooxidation of sucrose

4.1.5.1 On adatoms modified platinum electrodes.- The selective oxidation of sucrose is likely to lead to mono, di- and polycarboxylic acids. These derivatives have a potential application in detergents, to replace phosphates, due to their properties of non-toxicity, biocompatibility and biodegradability. Electrolysis of sucrose was performed in a filter press cell (Micro-Flow Cell, Electro-cell AB), (Figure 19).

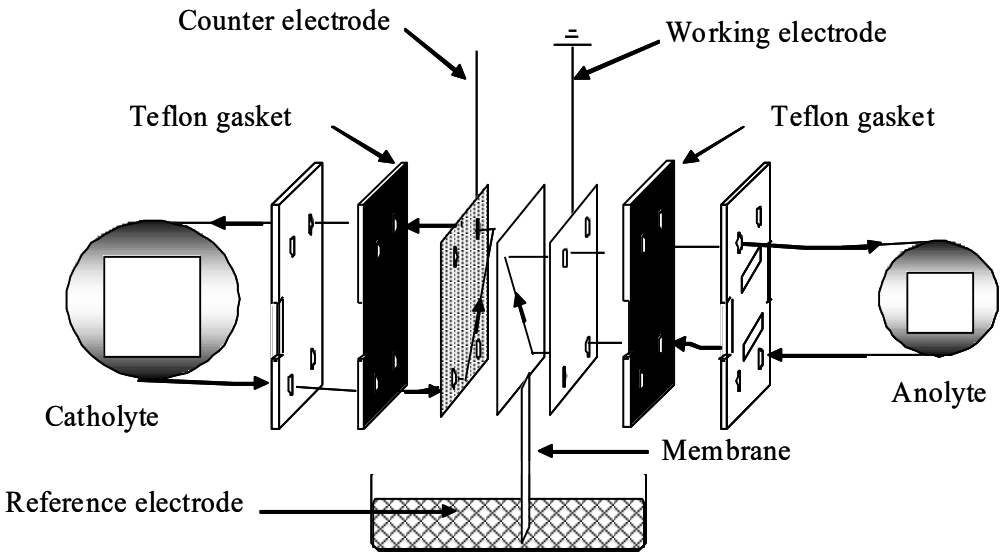

Figure 15: Schematic representation of the filter press cell used to carry out the electrooxidation of carbohydrates.

The working electrode was platinum deposited electrochemically on a titanium plate. The counter electrode was a plate of stainless steel. The two-compartments of the cell were separated by an ion-exchange membrane (Nafion® 423). A part of this membrane immersed in a saturated solution of K_2SO_4, permitted to connect, by capillarity, the mercury/mercurous sulfate reference electrode (MSE). The electrolyte in the cell was circulated by an external peristaltic pump (1 cm^3 min^{-1}) and passed through a reservoir (100 cm^3).

Some attempts[2] in alkaline solution (0.1 M NaOH) have shown an important current decay caused by the participation of the hydroxyl species of the electrolyte to the formation of carboxylates. Accordingly, the oxidation of sucrose was carried out on a lead modified platinum

[2] The electrochemical instrumentation consisted of an Hewlett Packard HP 33120A Arbitrary Waveform Generator coupled to a Bank High Power Potentiostat (Wenking Model HP88). The potential program is synthesized with an HP BenchLink Software (HP BenchLink/Arb) under a Windows™ environment, and then it is transferred to the function generator. Data such as applied potential, current intensity and quantity of electricity were acquired by a PC microcomputer equipped with an AD/DA convertor (Keithley DAS 20-Viewdac).

electrode, in 0.1 M Na_2CO_3-$NaHCO_3$ (Figure 20). During the positive variation of potential, two oxidation peaks of sucrose, A and B, are observed at 0.8 V *vs*. RHE (j = 0.8 mA cm^{-2}) and at 1.1 V *vs*. RHE (j = 0.44 mA cm^{-2}). During the negative variation of potential, another peak, C, is noticed at 0.7 V *vs*. RHE (j = 0.3 mA cm^{-2}) after desorption of the oxygenated species from the electrode surface.

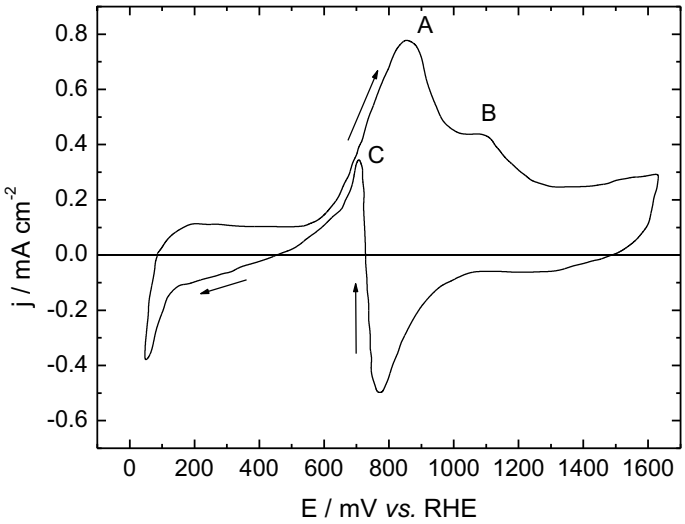

Figure 20: Voltammogram of a Pt-Pb electrode recorded in 0.1M Na_2CO_3-$NaHCO_3$ + 10.2 mM sucrose at 50 mV s^{-1}; $[Pb^{2+}] = 10^{-5}$ M.

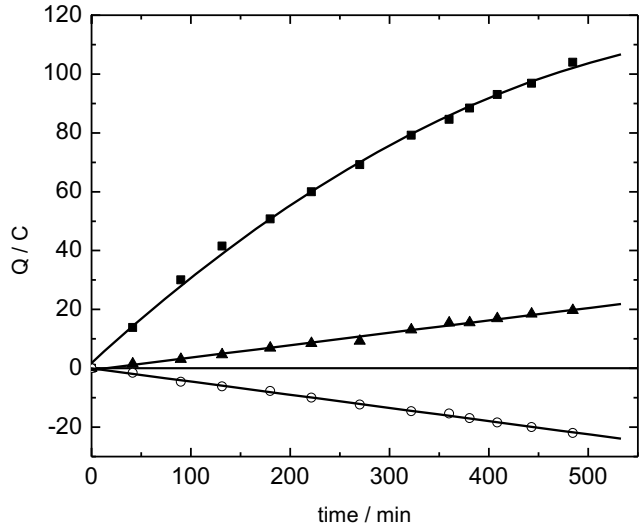

Figure 21: Variation of the quantity of electricity at each step potential of the time programme applied during the oxidation of sucrose on a Pt-Pb electrode.

The electrolysis of the same solution of sucrose was carried out under the same experimental conditions during 8.3 h with the potential program described in Figure 13. The oxidation pulse step was fixed at 0.74 V *vs*. RHE. The quantity of electricity at each potential plateau was evaluated and presented in Figure 17. It can be noted that Q_{des} and Q_{ads} show a quasi-symmetrical profile with a small advantage for Q_{ads}.

Q_{ads} is the quantity of electricity which served to adsorb the organic molecule and eventually to reduce the electrode surface.

As for Q_{des}, it can be assumed that this quantity of electricity allowed to clear out the electrode surface from the poisoning organic species. But, if the active surface of platinum was covered by OH_{ads} at the desorption plateau (1.63 V *vs*. RHE), after 8.3 h of electrolysis, $Q_{(OH)ads}$ would be estimated as followed:

$$Q_{(OH)ads} = n \times e \times (OH)_{ads} \times S_a \times \tau \qquad (21)$$

where n is the electron number (n = 1), e is the electron elementary charge, $(OH)_{ads}$, the number of adsorbed hydroxyls, i.e. the number of platinum sites per cm^2 ($1.35\ 10^{15}$); S_a is the active surface of the working electrode (45 cm^2) and τ is the number of cycles with t_{des} (0.2 s) used during the electrolysis ($\tau = 1852$), which gives: $Q_{(OH)ads}$= 17.34 C. This estimation is close to the experimental value (Q_{des} = 19.7 C). This means that the electrooxidation of sucrose took place at 0.74 V *vs*. RHE with nearly no poisoning species involved. The sole quantity of electricity, which served to oxidize sucrose, was thus Q_{ox}. At the end of electrolysis, this value was estimated to *ca*. 104 C and the yield of the sucrose transformation was estimated close to 60%. The solution was sampled and neutralized on a cation exchange resin (Amberlite 200, Sigma). The solutions obtained, free from inorganic cations (Na^+), were chromatographied again to be sure of the reproducibility of the last analysis.

The chemical shifts of the ^{13}C-NMR spectrum recorded in D_2O with methanol as an internal reference and in the presence of NaOH in order to keep the pH in the alkaline range and to prevent the lactone formation are given in Table 1.

Table 1: Chemical shifts of the ^{13}C NMR spectrum of the lyophilized reaction products obtained on a Pt-Pb electrode in comparison with sucrose used as reference.

δ(C)/ppm	C'1	C'2	C'3	C'4	C'5	C'6	C1	C2	C3	C4	C5	C6
Sucrose	63.3	104.4	77.4	75.0	82.2	63.4	92.9	72	73.6	70.2	73.3	61.1
1'-sucronic acid	183.2	106	78.6	77.7	81.5	62.9	93.7	72.7	74.5	70.8	73.4	61.6

The confirmation of the oxidation of the primary hydroxyl group located at C'_1 to a carboxylic acid group is based on the two peaks (at 62 and 63 ppm) in the (CH_2OH) region and on the peak at 183 ppm in the "carbonyl region" of the spectrum. This is in accordance with the interpretation of Eyde *et al*.[73].

All these analytical results are in agreement with the experimental number of electrons involved during prolonged electrolyses of sucrose, which were found to be very close to 4. This confirms that the oxidation of one primary alcohol group leads to one carboxylic acid group (which needs 4 electrons per alcohol group), either the 1'-MAS with a selectivity close to 80% or to the 6-MAS (with a selectivity close to 10%) on a upd-Pb/Pt electrode.[74-75]

4.1.6 Electrooxidation of lactose

Different voltammograms were recorded at various concentrations of metal adatoms (Pb, Bi and Tl) in the presence of 10 mM lactose in 0.1 M Na_2CO_3-$NaHCO_3$. Their optimized concentrations evidenced the electrocatalytic effect by the ratio $I_{Pt\text{-}M}/I_{Pt}$ for the current densities, with and without adatoms, *versus* electrode potential (Figure 22). In fact, the presence of the

metal adatoms at the Pt surface induces a shift of the lactose oxidation peaks towards lower potential and an increase in the current densities.

Using the previous information provided by the voltammetric measurements, the oxidation of 10 mM lactose was carried out in carbonate buffer and in the presence of lead adatoms ($[Pb^{2+}]$ = $5x10^{-6}$ M). Electrolysis was carried out in a two-compartment cell (2x70 cm^3) for 3 h by applying repeatedly the suitable triple pulse potential program. The oxidation potential was set to 0.6 V *vs.* RHE on a Pt electrode which had an active surface area of 18 cm^2. After 3h the recorded quantity of electricity, Q_{exp} = 15.1 C, showed that the lactose conversion yield was 87% and 90% of selectivity in lactobionate was obtained:[76-77]

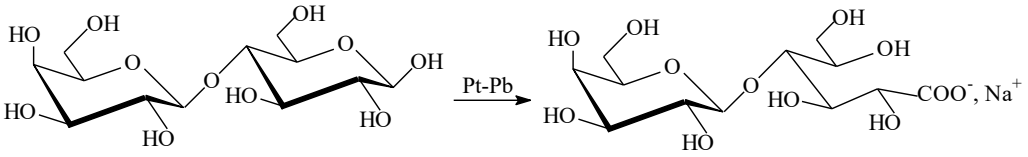

Lactose Lactobionate (22)

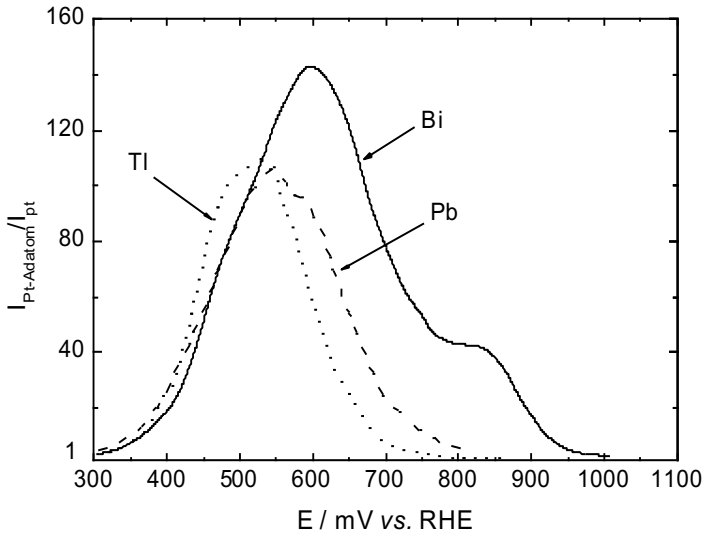

Figure 22: Electrocatalytic effect of metal adatoms on the lactose oxidation in carbonate buffer during the positive potential going scan. (—) with 5 x 10^{-6} mol L^{-1} bismuth; (-----) with 5 x 10^{-6} mol L^{-1} lead; (....) with 5 x 10^{-6} mol L^{-1} thallium.

Treatments of the electrolytic solution were required to remove carbonates with an exchange resin (Amberlite 200). Then a dry and solid material was recovered by lyophilization of water. Finally, the ^{13}C NMR spectrum of the reaction product was compared to that of lactose to determine the oxidized group (Table 2).

Table 2: Chemical shifts of the ^{13}C NMR spectrum of the lyophilized reaction product obtained on a Pt-Pb electrode in comparison with lactose used as reference.

δ(C)/ppm	**C'$_1$**	**C'$_2$**	**C'$_3$**	**C'$_4$**	**C'$_5$**	**C'$_6$**	**C$_1$**	**C$_2$**	**C$_3$**	**C$_4$**	**C$_5$**	**C$_6$**
Lactose	103.0	70.0	81.1	68.9	84.7	61.0	91.94	75.6	71.7	90.6	72.9	62.0
Lactobionic acid	103.6	70.8	72,5	68.5	75.2	60.8	**175.5**	71,5	71.0	80.6	71.4	61.9

4.1.7 Cathodic process: carbonyl compounds

Various methods have been used to produce selectively lactic acid or dimethyltartaric acid (or pinacol) by the reduction of pyruvic acid and its derivatives. The hydrogenation product (lactic acid) is a useful intermediate in the biological sector, food and polymer industries.[78]

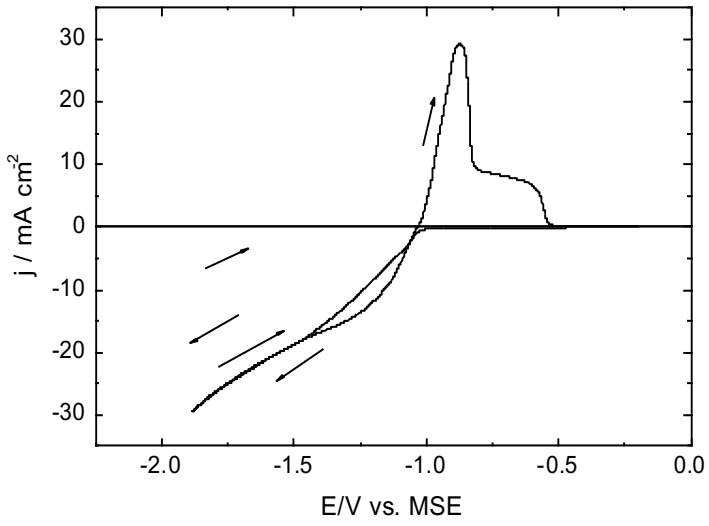

Figure 23: Voltammograms of a Pb electrode recorded at 50 mV s^{-1}; (---) in 0.5 M H_2SO_4 supporting electrolyte alone and (—) in the presence of 0.1 M pyruvic acid.

Cyclic voltammetry was used to check the degree of purity of the reaction medium (0.5 M H_2SO_4 or 0.5 M $NaHCO_3/Na_2CO_3$) and that of the electrode. In sulfuric acid (Figure 23), it can be seen during the positive potential scan, an oxidation peak at E = -0.8 V *vs*. $Hg/Hg_2SO_4/K_2SO_4$ sat (MSE: E_{MSE} = 0.650 V *vs*. RHE at pH=0). This peak followed by a shoulder is attributed to $PbSO_4$ species which desorbs irreversibly from the electrode surface at E = -1.05 *vs*. MSE. A reduction wave of pyruvic acid begins in 0.5 H_2SO_4 at *ca* -1.05 V *vs*. MSE where $PbSO_4$ desorbs from the electrode surface. In carbonate buffer (Figure 24), the electrode surface is oxidized at -1.02 V *vs*. MSE to $PbCO_3$ that were reduced reversibly during the negative potential sweep. In this medium, the reduction of pyruvic acid keeps the same shape, which starts at -1.65 V *vs*. MSE. Hydrogen evolution was observed at the lead cathode from -1.4 and -2.2 V *vs*. MSE according to the nature of the supporting electrolyte. Therefore, the production of the latter should be competitive with that of lactic acid and dimethyltartaric acid at more negative potentials.

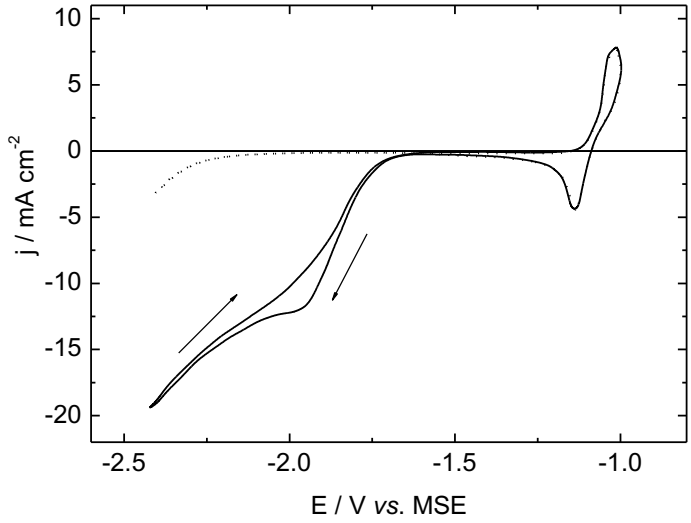

Figure 24: Voltammograms of a Pb electrode recorded at 50 mV s^{-1}; (---) in 0.5 M Na_2CO_3 + 0.5 M $NaHCO_3$ supporting electrolyte alone and (—) in the presence of 0.1 M pyruvate.

A series of electrolyses of pyruvic acid were carried out at different fixed potentials in an undivided conventional three-electrode Pyrex cell (50 cm^3). In sulphuric acid the electrohydrodimerization process was favoured (69%) when increasing the concentration of pyruvic acid and the electrode potential:

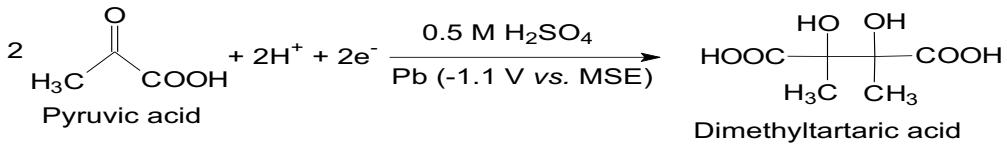

Pyruvic acid — Dimethyltartaric acid (23)

In carbonate buffer, the selectivity towards lactate was higher (90%) and seemed to be promoted when the electrode potential was set close to the hydrogen evolution reaction:

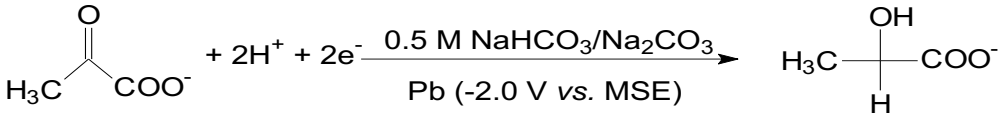

Pyruvate — Lactate (24)

Analyses of the electrolyzed solutions by HPLC[3] allowed to determine lactic and dimethyltartaric acids.[79-82] A chemical step of esterification is necessary to separate and isolate the reaction products.

[3] Analysis of the composition mixture was carried out by HPLC which consisted of a pump (Knauer Pump 64) and two detectors settled online (UV Applied Biosystems 785A and refractometer Shodex RI-71). The partition was performed on a HPX-87H (300 mm x 7.8 mm, BioRad, 3.33 mM H_2SO_4 in water, 0.6 mL min^{-1}) and the quantitative analyses were carried out using the so-called 'external standard' method. According to the used medium as supporting electrolyte, an ionic exchange resin was necessary to neutralize it (for the sulphuric acid solution: Amberlite IRA-900 Cl and for the alkaline solutions: Amberlite IRA-400 Na). The aqueous solutions of the electrolyzed products, free from inorganic ions, were removed at 50 °C under vacuum, and then dissolved in methanol (10 cm^3) for esterification using 2,2-dimethoxypropane (1 cm^3). The separation was performed on silica gel 15-40 μm (Silica Gel 60 from Sigma) with ethyl acetate/petroleum ether (60:40) as eluent.

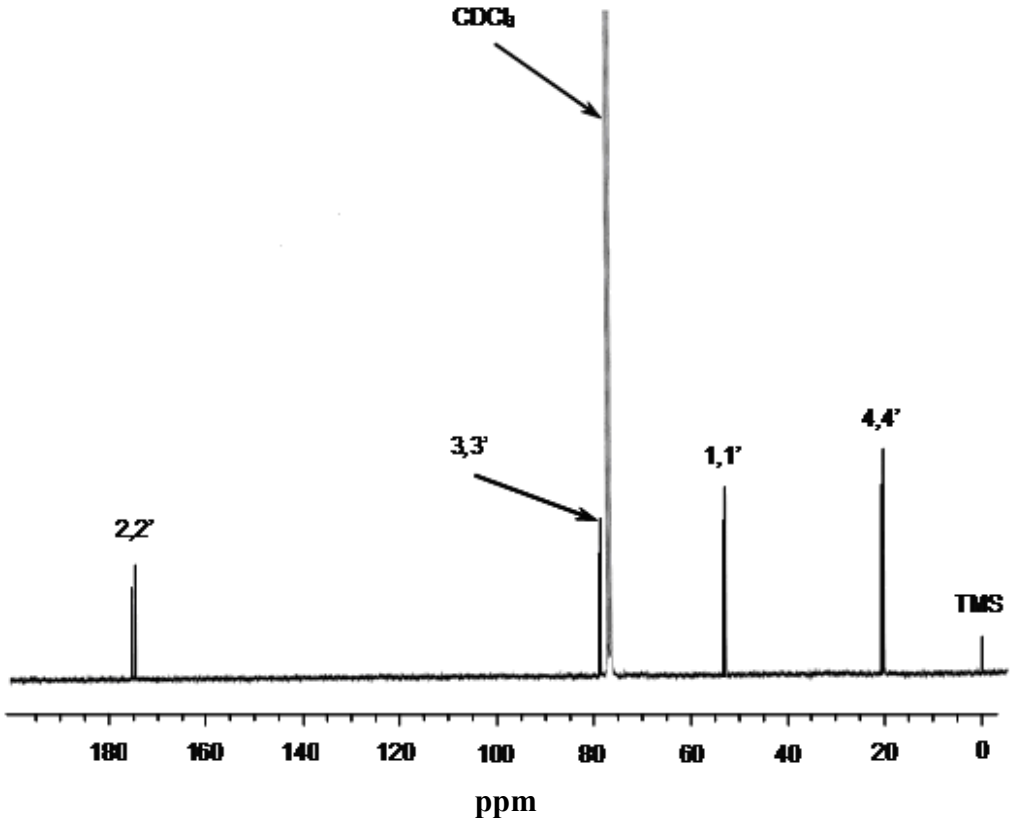

Figure 25: ^{13}C NMR spectrum of dimethylester of 2,3-dimethyltartaric acid in $CDCl_3$ obtained at the end of electrolysis of 0.1 M pyruvic acid at -1.1 V vs. MSE on lead cathode and after esterification. The internal reference is TMS.

However, the aqueous electrolyte was removed at the end of electrolysis to recover dry organic compounds free from inorganic ions. The esterified corresponding products were separated by flash chromatography and then identified spectroscopically by GC-MS-MS[4], and ^{13}C NMR[5] (Figure 25).

[4] The different reaction products were identified by GC-MS-MS (EI: 70 eV, CI/NH_3 and CI/CH_4: 100 eV, 1200L Varian).

[5] ^{13}C NMR: 300 MHz, $CDCl_3$, WP 200 SY Bruker spectrometer.

5. Summary and outlook

The basis of surface modification of electrodes surfaces by adatoms has been delineated by selected examples regarding the oxidation and reduction processes of small organic molecules in aqueous medium. The complex interplay of surface adatoms favors the electroactivity of a determined species and delivers some insights as to the mechanism of such organic molecules in favour of a product with an added value.

The future progress of organic activation via electrocatalysis can be associated with the development of the following topics:

- In the case of platinum and gold to find the optimum alloy combination in the nanoscale domain to enhance the glucose oxidation, which is the anodic reaction in a biofuel cell system, concomitant with surface defects control.[26, 83]
- Value added value products, such as the reduction of oxalic acid to glyoxylic acid are nowadays developed at an industrial scale (BASF- Badische Anilin und Soda-Fabriken). This process uses non-precious metals such as lead. This electrode material reduces carbon dioxide reduction to formic acid in aqueous medium and to oxalic acid in an organic solvent. This approach can be used to develop environmentally friendly value added products from abundant anthropogenic carbon dioxide.

Acknowledgements

The authors kindly acknowledge their students and collaborators for their contribution.

References

1. S. Trasatti, R. Parsons, *Pure Appl. Chem.*, **58**, (1986) 437.
2. E. Gileadi, *Electrode Kinetics for Chemists, Chemical Engineers, and Materials Scientists*, VCH: Weinheim, Germany, 1993.
3. V. S. Bagotskii and Y. B. Vasil'ev, *Electrochim Acta* 12 (1967) 1323.
4. B. D. McNicol, A. G. Chapman, R. T. Short, *J. Appl. Electrochem.*, **6**, 221 (1976).
5. L. D. Burke and O. J. Murphy, *J. Electroanal. Chem.* **101** (1979) 351.
6. C. Lamy, J. M. Leger, and J. Clavilier, *J. Electroanal. Chem.*, **135** (1982) 321.

7. T. Frelink, W. Visscher, J. A. R. van Veen, *J. Electroanal. Chem.*, **382** (1995) 65.
8. Z. D. Wei, L. L. Li, Y. H. Luo, C. Yan, C. X. Sun, G. Z. Yin, P. K. Shen, *J. Phys. Chem. B*, **110**, (2006) 26055.
9. A. S. Arico, P. Creti, N. Giordano, V. Antonucci, P. L. Antonucci, A. Chuvilin, *J. Appl. Electrochem.*, **26** (1996) 959.
10. G. Bronoel, S. Besse, N. Tassin, *Electrochim. Acta*, **37** (1992) 1351.
11. T. Iwasita and W. Vielstich, *J. Electroanal. Chem.*, **201** (1986) 403.
12. A. S. Lin, A. D. Kowalak, and W. E. O'Grady, *J. Power Sources*, **58** (1996) 67.
13. H. Hitmi, E. M. Belgsir, J. M. Léger, C. Lamy, and R. O. Lezna, *Electrochim. Acta*, **39** (1994) 407.
14. J. P. I. Souza, F. J. Botelho Rabelo, I. R. de Moraes, and F. C. Nart, *J. Electroanal. Chem.*, **420**, (1997) 17.
15. F. Delime, J.-M. Leger, C. Lamy, *J. Appl. Electrochem.*, **29** (1999) 1249.
16. D. T. Shieh and B. J. Hwang, *J. Electrochem. Soc.*, **142** (1995) 816.
17. X. Xue, J. Ge, T. Tian, C. Liu, W. Xing, T. Lu, *J. Power Sources*, **172** (2007) 560.
18. I. G. Casella, M. Gatta, M. Contursi, *J. Electroanal. Chem.*, **561** (2004) 103.
19. S. Berchmans, H. Gomathi, G. P. Rao, *J. Electroanal. Chem.*, **394** (1995) 267.
20. T. R. I. Cataldi, A. Guerrieri, I. G. Casella, E. Desimoni, *Electroanalysis*, **7** (1995) 305.
21. H. S. Liu, C. J. Song, L. Zhang, J. J. Zhang, H. J. Wang, D. P. Wilkinson, *J. Power Sources*, **155** (2006) 95.
22. M. Baldauf, W. Preidel, *J. Power Sources*, **84** (1999) 161.
23. P. Atanassov, C. Apblett, S. Banta, B. Susan, S. C. Barton, M. Cooney, B. Y. Liaw, S. Mukerjee, and S. D. Minteer, *Electrochem. Soc. Interface*, **16** (2007) 28.
24. A. Habrioux, K. Servat, B. Kokoh, and N. Alonso-Vante, *ECS Trans.*, **6**, 9 (2007).
25. A. Habrioux, E. Sibert, K. Servat, W. Vogel, K. B. Kokoh, and N. Alonso-Vante, *J. Phys. Chem. B*, **111** (2007) 10329.
26. K. L. Hsueh, E. R. Gonzalez, and S. Srinivasan, *Electrochim. Acta*, **28** (1983) 691.
27. A. Damjanovic, M. A. Genshaw, and J. O'M Bockris, *J. Chem Phys*, **45** (1966) 4057.
28. H. S. Wroblowa, P. Yen Chi, and G. Razumney, *J. Electroanal. Chem.*, **69** (1976) 195.
29. G. Tamizhmani, J. P. Dodelet, D. Guay, *J. Electrochem. Soc.*, **143** (1996) 18.
30. N. M. Markovic, T. J. Schmidt , V. Stamenkovic, and P. N. Ross, *Fuel Cells*, **1** (2001) 105.
31. P. N. Ross, *J. Electrochem. Soc.*, **126** (1979) 78.
32. P. Fischer, J. Heitbaum, *J. Electroanal. Chem.*, **112** (1980) 231.
33. K. J. J. Mayrhofer, B. B. Blizanac, M. Arenz, V. R. Stamenkovic, and P. N. Ross, N. M. Markovic, *J. Phys. Chem. B*, **109** (2005) 14433.
34. V. Komanicky, A. Menzel, and H. You, *J. Phys. Chem. B*, **109** (2005) 23550.
35. K. Kinoshita, *J. Electrochem. Soc.*, **137** (1990) 845.
36. N. Alonso-Vante, *Pure Appl. Chem.*, **80** (2008) 2103.
37. J. Giner, L. Marincic, J. S. Soeldner, and C. K. Colton, *J. Electrochem. Soc.*, **128** (1981) 2106.
38. F. Largeaud, K. B. Kokoh, B. Beden, C. Lamy, *J. Electroanal. Chem.*, **397** (1995) 261.
39. H. Angerstein-Kozlowska, *Surfaces, Cells, and Solutions for Kinetics Studies*, Plenum Press: New York, 1984.
40. B. E. Conway and L. Bai, *J. Electroanal. Chem.*, **198** (1986) 149.
41. A. J. Appleby. Electrocatalysis. In *Modern Aspects of Electrochemistry*, B. E. Conway andJ. O. M. Bockris, Eds. Plenum Press: New York, 1974.
42. D. Zurawski, L. Rice, M. Hourani, and A. Wieckowski, *J. Electroanal. Chem.*, **230** (1987) 221.
43. A. N. Kahyaoglu. Oxydation électrocatalytique du glycérol sur le platine, l'or et leurs

alliages binaires, PhD, Poitiers, 1981.
44. H. Möller, P. C. Pistorius, *J. Electroanal. Chem.*, **570** (2004) 243.
45. R. R. Adzic, N. M. Markovic, *Electrochim. Acta*, **30** (1985) 1473.
46. N. Furuya, S. Motoo, *J. Electroanal. Chem.*, **98** (1979) 189.
47. R. Gomez, J. M. Feliu, *J. Electroanal. Chem.*, **554-555** (2003) 145.
48. G. Kokkindis, J. M. Léger, C. Lamy, *J. Electroanal. Chem.*, **242** (1988) 221.
49. G. Kokkinidis, D. Sazou, I. Moumtzis, *J. Electroanal. Chem.*, **213** (1986) 135.
50. F. Matsumoto, M. Harada, N. Koura, S. Uesugi, *Electrochem. Commun.*, **5**, 42 (2003).
51. S. Motoo, and N. Furuya, *J. Electroanal. Chem.*, **184** (1985) 303.
52. M. Sakamoto, K. Takamura, *Bioelectrochem Bioenerg*, **9** (1982) 571.
53. M.-J. Shao, X.-K. Xing, C.-C. Liu, *Bioelectrochem Bioenerg*, **17** (1987) 59.
54. M. Shibata, N. Furuya, M. Watanabe, S. Motoo, *J. Electroanal. Chem.*, **263** (1989) 97.
55. P. C. C. Smits, B. F. M. Kuster, K. van der Wiele, S. van der Baan, *Appl Catal*, **33** (1987) 83.
56. M. Watanabe, M. Horiuchi, S. Motoo, *J. Electroanal. Chem.*, **250** (1988) 117.
57. C. Paul Wilde, M. Zhang, *Electrochim. Acta*, **38** (1993) 2725.
58. Q.-H. Wu, S.-G. Sun, X.-Y. Xiao, Y.-Y. Yang, Z.-Y. Zhou, *Electrochim. Acta*, **45** (2000) 3683.
59. G. Kokkinidis, N. Xonoglou, *Bioelectrochem. Bioenerg.*, **14** (1985) 375.
60. B. Beden, J.-M. Léger, C. Lamy, *Electrocatalytic Oxidation of Oxygenated Aliphatic Organic Compounds at Noble Metal Electrodes*, Plenum Press: New York, 1992.
61. S. Ernst, C. H. Hamann, J. Heitbaum, *Ber. Bunsen-Ges. Phys. Chem.*, **84** (1980) 50.
62. H.-W. Lei, B. Wu, C.-S. Cha, H. Kita, *J. Electroanal. Chem.*, **382** (1995) 103.
63. L. H. E. Yei, B. Beden, C. Lamy, *J. Electroanal. Chem.*, **246** (1988) 349.
64. B. Beden, F. Largeaud, K. B. Kokoh, C. Lamy, *Electrochim. Acta*, **41** (1996) 701.
65. M. L. F. De Mele, H. A. Videla, A. J. Arvia, *Bioelectrochem Bioenerg*, **16** (1986) 213.
66. M. Fleischmann, Z. Q. Tian, *J. Electroanal. Chem.*, **217** (1987) 385.
67. M. W. Hsiao, R. R. Adzic, E. B. Yeager, *Electrochim. Acta*, **37** (1992) 357.
68. M. W. Hsiao, R. R. Adzic, E. B. Yeager, *J. Electrochem. Soc.*, **143** (1996) 759.
69. K. B. Kokoh, J. M. Léger, B. Beden, H. Huser, C. Lamy, *Electrochim. Acta*, **37** (1992) 1909.
70. L. A. Larew, D. C. Johnson, *J. Electroanal. Chem.*, **262** (1989) 167.
71. N. N. Nikolaeva, O. A. Khazova, Y. B. Vassilyev, *Elektrokhimiya*, **18** (1982) 1120.
72. L. A. Edye, G. V. Meehan, G. N. Richards, *J. Carbohydr. Chem.*, **10** (1991) 11.
73. P. Parpot, K. B. Kokoh, B. Beden, C. Lamy, *Electrochim. Acta*, **38** (1993) 1679.
74. P. Parpot, K. B. Kokoh, E. M. Belgsir, J. M. Léger, B. Beden, C. Lamy, *J. Appl. Electrochem.*, **27** (1997) 25.
75. H. Druliolle, K. B. Kokoh, B. Beden, *Electrochim. Acta*, **39** (1994) 2577.
76. H. Druliolle, K. B. Kokoh, F. Hahn, C. Lamy, B. Beden, *J. Electroanal. Chem.*, **426** (1997) 103.
77. M. Atobe, T. Nonaka, *Chem. Lett.*, **24** (1995) 669.
78. K. Matsuda, M. Atobe, T. Nonaka, *Chem. Lett.*, **23** (1994) 1619.
79. C. Martin, H. Huser, K. Servat, K. B. Kokoh, *Electrochim. Acta*, **50** (2005) 2431.
80. C. Martin, H. Huser, K. Servat, K. B. Kokoh, *Tetrahedron Lett.*, **47** (2006) 3459.
81. C. Martin, K. Servat, H. Huser, K. B. Kokoh, *J. Appl. Electrochem.*, **36** (2006) 643.
82. A. Habrioux, K. Servat, S. Tingry, and K. B. Kokoh, *Electrochem. Commun.*, **11** (2008) 111.
83. A. Habrioux, W. Vogel, M. Guinel, L. Guetaz, K. Servat, K. B. Kokoh, and N. Alonso-Vante, *Phys. Chem Chem Phys*. **11** (2009) 3573.